An Optical-driven Method for PolSAR Feature Extraction

Yi Zhao[1], Mi Jiang[1,2,*], Zhangfeng Ma[1]

[1] School of Earth Sciences and Engineering, Hohai University, Nanjing, People's Republic of China;

[2] State Key Laboratory of Hydrology-Water Resources and Hydraulic Engineering, Hohai University, Nanjing, People's Republic of China;

* Corresponding author: mijiang@hhu.edu.cn

Introduction

PolSAR data has become the significant data source in urban research. However, the speckle in SAR images introduces biases into polarimetric feature estimation and brings challenges to the interpretation of land covers. Widely used methods suppress the speckle and extract features at the expense of spatial resolution loss [1]. A novel optimized method driven by optical images is addressed to preserve the complicated structures and obtain accurate polarimetric features.

Method

The speckle effects not only the intensity information but also the correlations between polarizations. Hence, the speckle ought to be reduced by averaging homogeneous samples of the covariance matrices $\boldsymbol{C}$ [2]. Inspired by previous studies [3-5], authors take use of spectral and polarimetric information to select neighborhood samples. The key to this algorithm is in which way the two kinds of characteristics are combined.

First of all, the similarity measurements for optical (dis_{opt}) and SAR (dis_{SAR}) are defined respectively (Eq.1, 2).

$$dis_{opt}(x,x') = \sqrt{\sum_{i=1}^{N}\left(x_i - x_i'\right)^2} \quad (1)$$

where x and x' denote the observation of the i^{th} band for center pixel and its neighborhoods.

$$dis_{SAR}(x,x') = \ln Q = n\left(2q\ln 2 + \ln|\boldsymbol{C}_x| + \ln|\boldsymbol{C}_{x'}| - 2\ln|\boldsymbol{C}_x + \boldsymbol{C}_{x'}|\right) \quad (2)$$

where $\boldsymbol{C}_x$ and $\boldsymbol{C}_{x'}$ denote the covariance matrices of x and x'.

Then, a Gaussian kernel is applied to combine both similarity.

$$p_i = \exp\left(\frac{-|dis_i|}{h}\right), i = opt \text{ or } SAR \quad (3)$$

where h controls the decay of the exponential function.

In order to avoid the use of experimental parameters we set h = 1 for both datasets and unify their scales through a linear transformation

$$\tilde{p}_i = \frac{p_i - \min(p_i)}{\max(p_i) - \min(p_i)} \quad (4)$$

Since the derived probabilities are independent of each other, their joint probability equals the product of the probability from both datasets.

$$\tilde{p}_{joint} = \tilde{p}_{opt} \cdot \tilde{p}_{SAR} \quad (5)$$

Finally, a nonparametric Otsu's segmentation is applied to derive a threshold. Pixels whose probability is below the threshold are selected as homogeneous samples. With those samples, the coherence matrix is estimated using local linear minimum mean square error (LLMMSE) method, and the estimator of polarimetric feature is also enhanced.

Results

Seninel-1/2 images over three reprehensive sites are shown in Fig.1, including rural (Fig.1.a,d), airport (Fig.1.b,e) and urban (Fig.1.c,f) area.

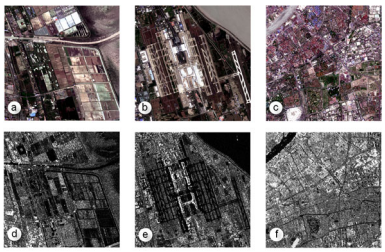

Fig. 1. Optical (a-c, RGB band: band 4,3,2) and SAR (d-f, VV+VH) images over three study areas.

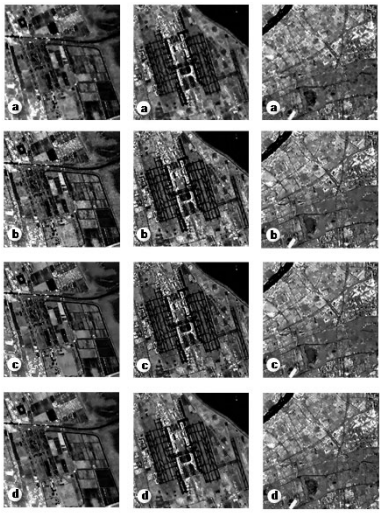

Fig. 2. Results over three regions filtered by (a) Refined Lee (b) IDAN (c) NL-SAR (d) Optical-Driven.

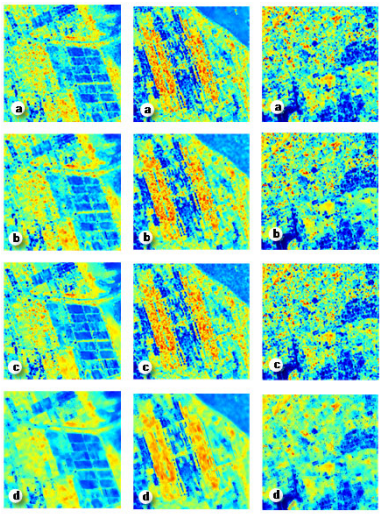

Fig. 3. Entropy parameter derived from filtered covriance in Fig.2. using different estimators: (a)-(c) boxcar estimator, (d) optical-driven estimator

Tab. 1. Quantitative evaluation of four filters over three study cites

	Rural			Airport			Urban		
	ENL	$\|\rho\|$	$\arg(\rho)$	ENL	$\|\rho\|$	$\arg(\rho)$	ENL	$\|\rho\|$	$\arg(\rho)$
Span image	2.89	0.11	1.98	4.04	0.72	2.24	0.29	0.16	0.85
Refine Lee	7.23	0.13	1.97	15.24	0.83	2.25	0.42	0.18	0.76
IDAN	7.96	0.12	2.12	15.80	0.81	2.39	0.44	0.18	0.99
NL-SAR	9.25	0.57	2.55	**38.58**	0.72	2.75	0.45	0.18	0.85
Optical-Driven	**10.68**	**0.12**	**2.03**	35.23	**0.73**	**2.30**	**0.46**	**0.16**	**0.92**

Fig.2 illustrates the span images filtered by different methods. Although all methods suppress the effect of speckle to varying extents, it is obvious that Refine Lee filter causes blurring and impairs the spatial resolution severely. Other filters obtain the more flexible results, but their performances vary among test sites.

The polarimetric feature Entropy derived by H-alpha decomposition is taken for detailed analyses due to its sensitivity to the speckle and multilooking effects. The parameter is usually extracted with a boxcar estimator, while the homogeneous samples are used as the optimized estimator. The results are shown in Fig.3.

Quantitatively, the equivalent number of looks (ENL) and complex correlation are calculated to further evaluate the performance (Tab. 1.).

Conclusions

A novel method driven by optical images to suppress the speckle in PolSAR data is proposed. Experimental results demonstrated its efficiency in speckle reduction and polarimetric feature extraction.

The new method relies on the homogeneous samples. To fulfill the adaptive selection with few parameters, optical and SAR information is combined through a statistical approach.

Compared to the commonly used method, the optical-driven filter is outstanding in maintaining the spatial resolution and preserving the detailed structures, especially over regions with rich texture. The joint use of optical images enhances not only intensity but also the polarimetric features. With the increasing uses of multi-sensor datasets, this paper provides a meaningful exploration for future applications.

References

[1] J.-S. Lee and E. Pottier, *Polarimetric radar imaging: from basics to applications*. CRC press, 2009.

[2] J.-S. Lee, T. L. Ainsworth, Y. Wang, and K.-S. Chen, "Polarimetric SAR speckle filtering and the extended sigma filter," *IEEE Transactions on geoscience and remote sensing,* vol. 53, no. 3, pp. 1150-1160, 2015.

[3] L. Verdoliva, R. Gaetano, G. Ruello, and G. Poggi, "Optical-driven nonlocal SAR despeckling," *IEEE Geoscience and Remote Sensing Letters,* vol. 12, no. 2, pp. 314-318, 2015.

[4] W. Ni and X. Gao, "Despeckling of SAR Image Using Generalized Guided Filter With Bayesian Nonlocal Means," *IEEE Transactions on Geoscience and Remote Sensing,* vol. 54, no. 1, pp. 567-579, 2016.

[5] K. He, J. Sun, and X. Tang, "Guided Image Filtering," *IEEE Transactions on Pattern Analysis and Machine Intelligence,* vol. 35, no. 6, pp. 1397-1409, 2013.

河海大學 HOHAI UNIVERSITY